

## Tomography of AM Her and QQ Vul

A. Staude, A.D. Schwope, P. Hedelt, A. Rau

*Astrophysikalisches Institut Potsdam, An der Sternwarte 16, 14482  
Potsdam, Germany*

R. Schwarz

*Universitäts-Sternwarte Göttingen, Geismarlandstr. 11, 37083  
Göttingen, Germany*

**Abstract.** We present optical high-resolution spectroscopy of AM Her and QQ Vul. Making use of indirect imaging techniques (Doppler and Roche tomography), we are able to make details visible, which a model of these systems has to be able to account for. Especially the emission line data cannot be explained by current models of polars.

### 1. Introduction

Although it is the prototype-polar, there had been no high-resolution optical spectroscopy of AM Her in the literature recently. To fill this gap and to get data of a quality already available for much fainter objects, we observed AM Her with the double-beam spectrograph TWIN at the 3.5m-telescope at Calar Alto (Spain) on June 5 and 6, 2000. We also observed QQ Vul (on June 4 and 7), for which there is some optical spectroscopy published (Schwope et al. 2000). But in this system the trailed spectra and tomograms looked different whenever observations were performed.

The spectral resolution we achieved is  $1.1 \text{ \AA}$  ( $\sim 80 \text{ km s}^{-1}$ ) between 4000 and 5000  $\text{\AA}$ , and  $1.4 \text{ \AA}$  ( $\sim 50 \text{ km s}^{-1}$ ) from 7660 to 8650  $\text{\AA}$ . Of AM Her we got 140 blue spectra with a time resolution of 140 s and 100 red spectra with a resolution of 200 s. In the case of QQ Vul we got 70 red spectra with 320 s resolution and 130 blue spectra with 200s resolution.

Parallel to the observations in Spain we observed the systems with the 0.7m-telescope at the AI Potsdam (Staude et al. 2000), to get photometric data in B and I band for photometric calibration of the spectra.

### 2. AM Her

The Sodium lines of AM Her (see Figure 1) show a sinusoidal motion and a change in intensity during one orbit. From a part of the data an improved ephemeris was derived already by Schwarz et al. (2001).

In addition to Doppler-tomography, giving an intensity map of the spectral line projected onto the orbital plane, we applied a mapping technique called

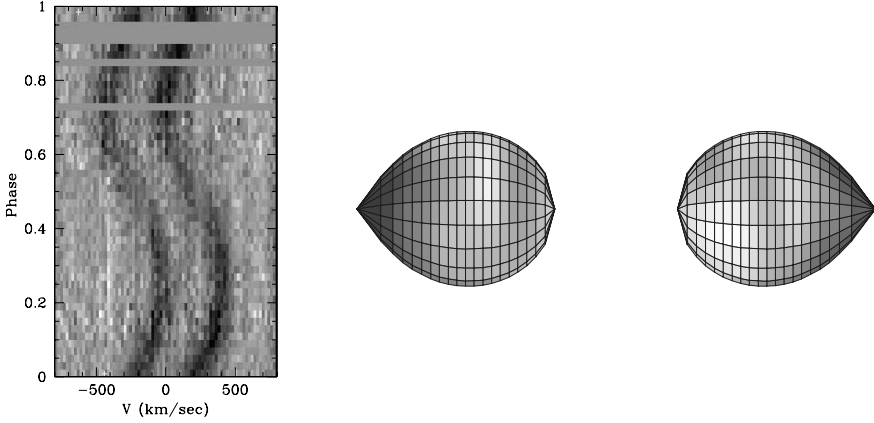


Figure 1. AM Her: NaI-lines and Roche-tomogram,  $Q=1.67$ ,  $M_1=0.433$ ,  $i=60^\circ$  (left: phase 0.25, right: phase 0.75, bright means stronger lines)

Roche-tomography (see e.g. Rutten et al. 1994) to the data, which calculates a map of the intensity on the surface of the secondary. We used our own code, which utilises evolution strategy (see e.g. Rechenberg 1994) for optimising the fit. By defining a ‘best-fit’ criterion (e.g. smoothness of the map), one can in principle determine the system parameters  $i$ ,  $Q$ , and  $M_1$ , assuming that these result in the smoothest map.

The Roche-tomogram shows depleted NaI-absorption on the X-ray irradiated side of the secondary. It seems that there is stronger absorption on the leading (visible at phase 0.75) than on the trailing side, which could be caused by shielding of the incident radiation by the accretion stream. The significance of further details in the map has to be tested with model data.

In Figure 2 the  $H\beta$  emission line shows a bright narrow component (NEL) and a diffuse stream contribution without substructure. In the resulting Doppler-tomogram the NEL is located at the expected position of the irradiated hemisphere of the secondary star. The remaining emission does not show a clear signature of the ballistic stream.

The trailed spectrum and the tomogram of HeII look different. The NEL is not centered on the secondary’s surface, which could denote that there is shielding of the incident radiation by the accretion stream. The observed structure in the tomogram resembles a stream but cannot be identified with a ballistic stream starting at  $L_1$ . Hence, our observations suggest modifications to the Roche-lobe overflow model. As is demonstrated in Figure 4, velocity components out of the orbital plane ( $v_z$ ) cannot be neglected when the system’s inclination is much lower than 90 degrees, i.e. in non-eclipsing systems. So a possible explanation for the observed tomograms appears: the accretion stream starts with  $v_z \neq 0$ , but not from  $L_1$ , since from there large deviations from  $v = 0$  are unlikely, but somewhere else on the secondary’s surface. To reach the Roche-lobe of the white dwarf, the matter either has to have a very high velocity component in the direction of the white dwarf, or has to be channelled towards it – for instance by a magnetic field.

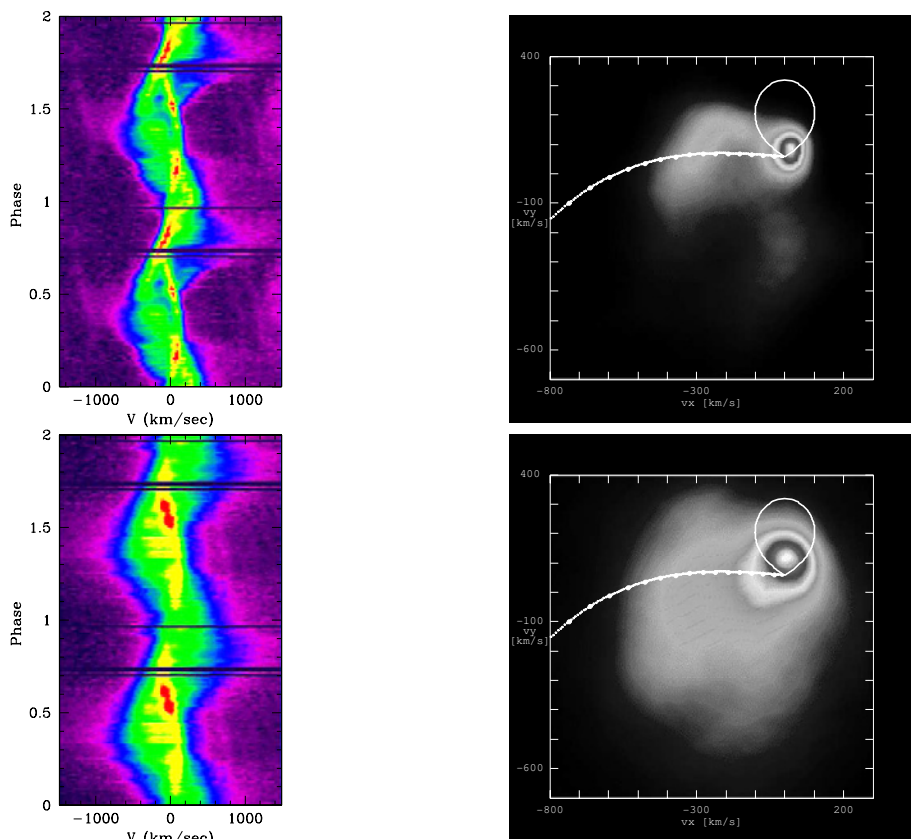


Figure 2. AM Her: trailed spectra and Doppler tomograms of HeII (top) and H $\beta$  (bottom) (Aug. 6), (Roche lobe and ballistic stream for  $Q=1.67$ ,  $M_1=0.433$  (Davey & Smith 1996),  $i=60^\circ$ )

In Figure 5 a scenario is shown, in which matter starts from the surface of the secondary quite far away from  $L_1$  with not vanishing  $v_z$ , and immediately couples onto a dipole fieldline of the white dwarf. It can be thought of as a very simple model for matter ejected from the secondary by a prominence.

### 3. QQ Vul

By fitting a sine-curve to the motion of the sodium doublet (Figure 6), spectroscopic phase zero was determined for the epoch of our observations.

In the Roche-tomogram the irradiated hemisphere of the secondary shows a depletion of the sodium absorption.

The trailed spectra of the emission lines (Figure 3) look different from the ones shown by Schwope et al. (2000). The tomograms of HeI $\lambda$ 4921, HeII $\lambda$ 4686, and H $\beta$  show a NEL and emission from the accretion stream. But the ratios

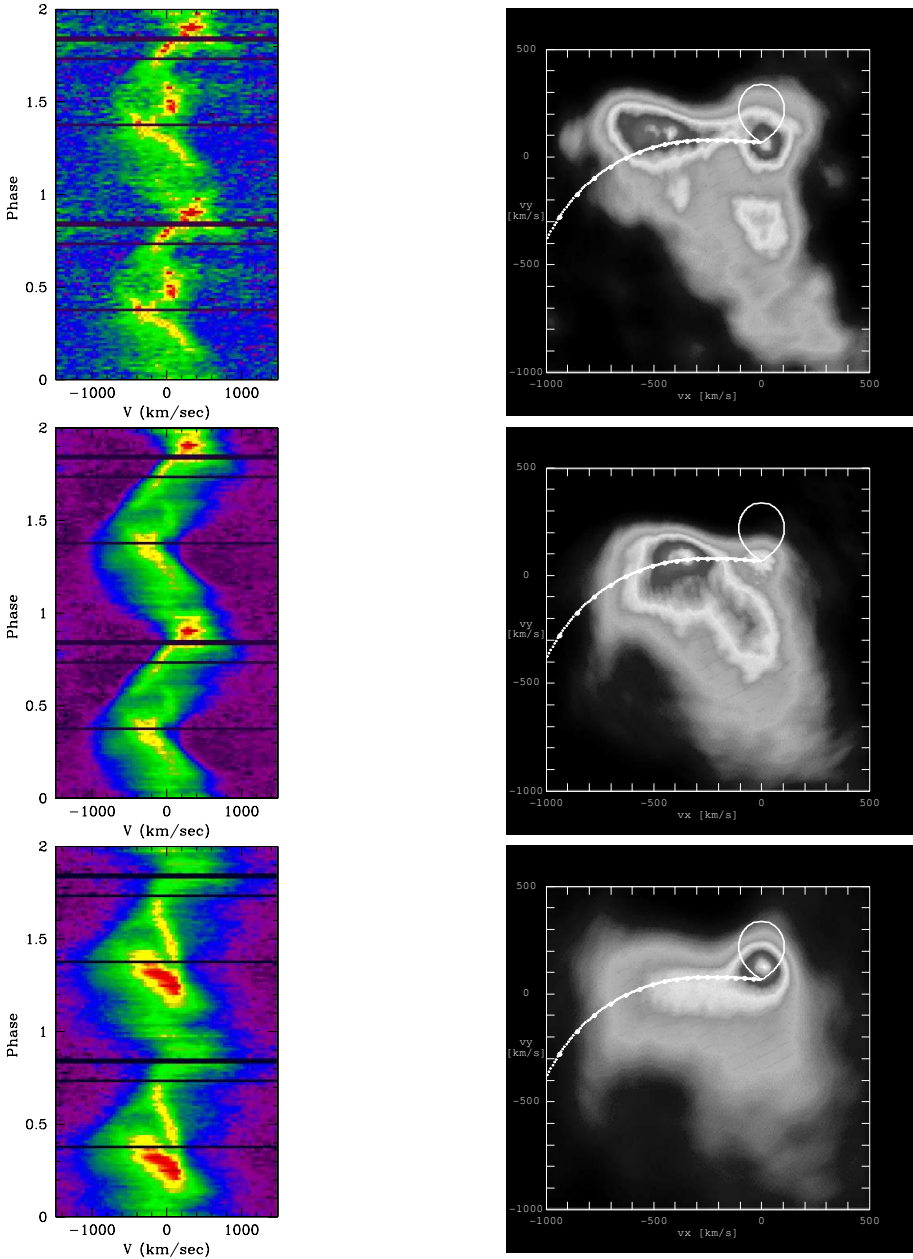


Figure 3. QQ Vul: trailed spectra and Doppler tomograms of HeI $\lambda$ 4921 (top), HeI $\lambda$ 4686 (middle) and H $\beta$  (bottom) (Roche lobe and ballistic stream for  $Q=1.75$ ,  $M_1=0.54$ ,  $i=65^\circ$  (Schwope et al. 2000))

between these components and the intrinsic shape of the stream emission is different for all species.

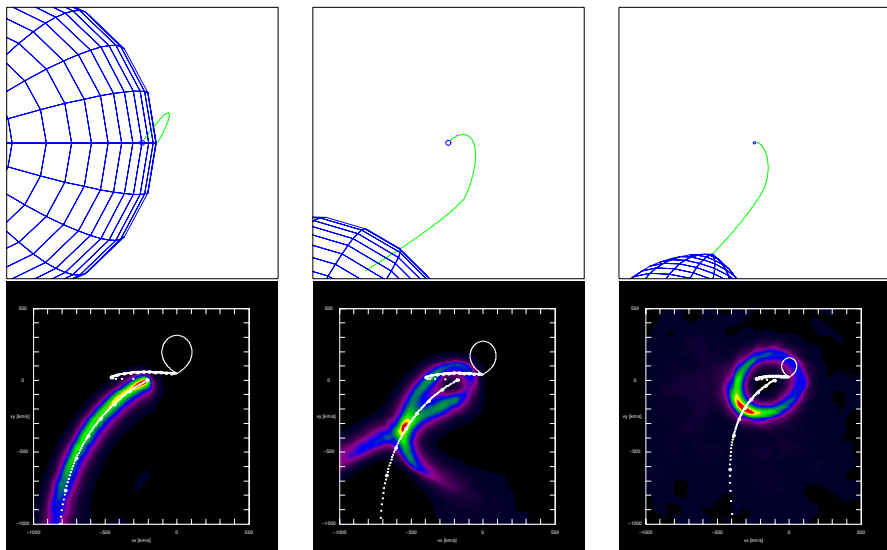


Figure 4.  $v_z$ -effects: Tomograms calculated from synthetic line spectra of the magnetically guided stream for  $i = 90^\circ, 60^\circ, 30^\circ$ .

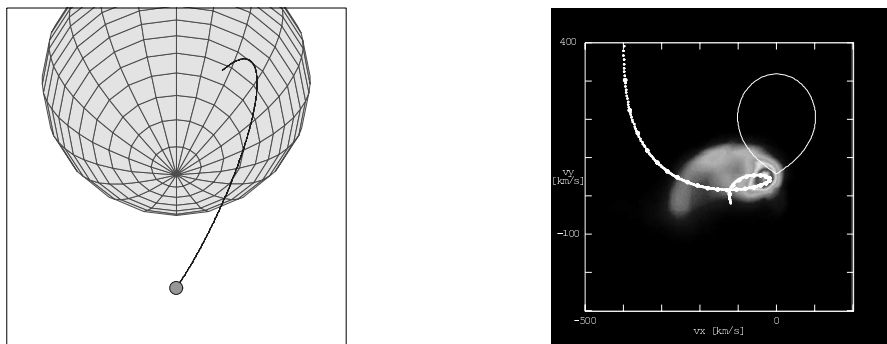


Figure 5. AM Her: A possible scenario which creates a synthetic tomogram similar to the observed one (same parameters as for Figure 3). An emission ratio of 3:1 of irradiated to unirradiated side was applied.

Both atomic species (H and HeI) show a relatively bright NEL, while it is almost completely overshadowed by the stream in the case of HeII. The reason could be that almost no X-ray radiation reaches the secondary, so that the Helium cannot be ionised.

While the Doppler-tomogram of  $H\beta$  shows mainly emission distributed homogeneously along the expected ballistic stream down to  $v_x \sim -800 \text{ km s}^{-1}$ , the stream emission in the other cases shows more substructure. There is a peak on the calculated position of the ballistic stream around  $v_x \sim -500 \text{ km s}^{-1}$  for HeI and around  $v_x \sim -400 \text{ km s}^{-1}$  for HeII. This could mark the stagnation

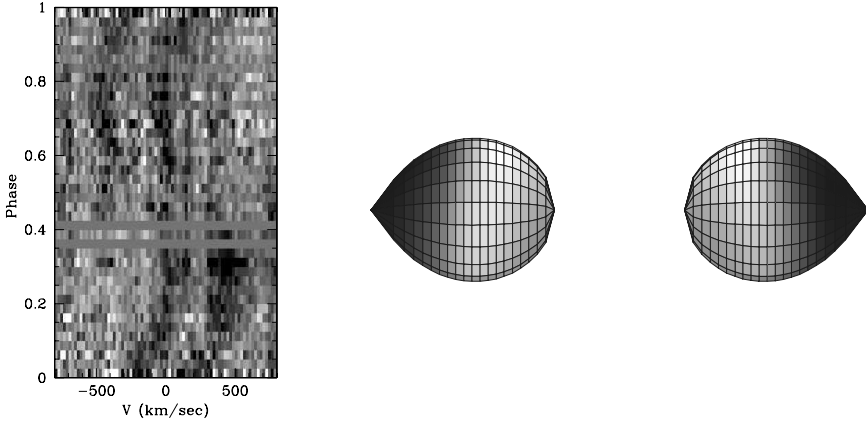


Figure 6. QQ Vul: NaI-lines and Roche-tomogram, calculated for  $Q=1.75$ ,  $M_1=0.543$ ,  $i=65^\circ$

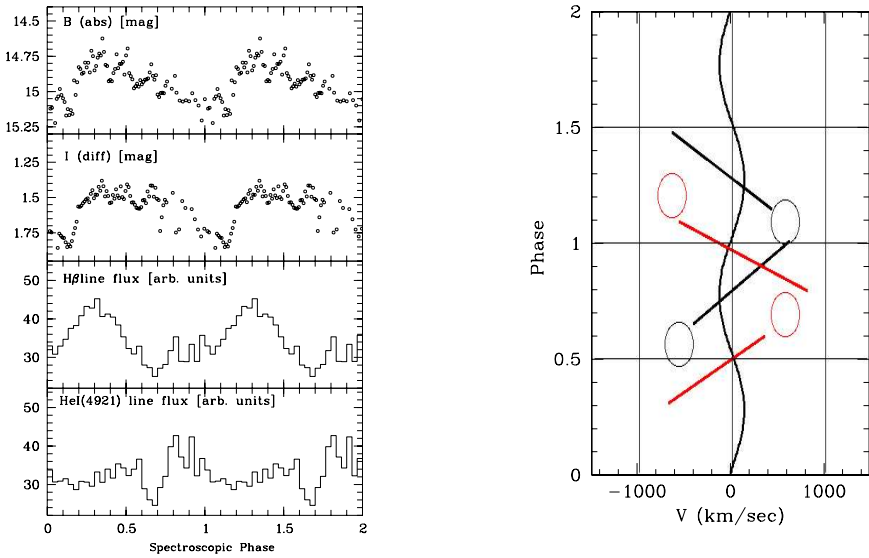


Figure 7. QQ Vul: *left*: Light curves, *right*: Schematic trailed spectrum: The positions of the features from the tomograms in the spectra: sine-curve = NEL, black lines = stagnation region, gray lines =  $v_x = 0$ -component, circles = regions with no emission from the components.

region, where the kinetic energy of the stream is partially transformed into radiation. To understand these findings and the absence of a visible stagnation region in the  $H\beta$ -tomogram, it will be necessary to involve radiation transport and magneto-hydrodynamics in the modelling of the accretion process.

Another interesting feature is the emission at  $v_x \sim 0$  and  $v_y \sim -300$  km s<sup>-1</sup> km s<sup>-1</sup> in the He maps. Since it has no  $v_x$ , the emission is arising from matter moving perpendicular to the connecting line of both stars – probably the magnetically guided stream.

The positions of the tomogram's features in the trailed spectra are shown schematically in Figure 7. The circles drawn there show where there is a lack of emission from the two parts of the stream, possibly caused by their small projected area.

The light curves (also Figure 7) of H $\beta$  and HeI both show a minimum around phase 0.6. But the maxima are at different phases: the ballistic stream in H $\beta$  is brightest before phase 0.5, when the irradiated side is visible. HeI is brightest after phase 0.5, meaning that the unirradiated side is brighter than the irradiated one.

#### 4. Conclusions

The emission line data of AM Her show details which are likely not compatible with the standard Roche-lobe overflow model. We suggest a model with the accretion stream starting somewhere else than  $L1$  from the secondary, taking effects of non-vanishing  $v_z$  into account.

The emission lines of QQ Vul again look different from those observed in the past. Also the minimum in the optical broad-band light-curves (Figure 7) is shifted from phase 0.95 in 1988 to  $\sim 0.1$  in our data. This can be a hint to a slight asynchronism. However, as pointed out by several speakers during the conference, the magnetic fields of the white dwarfs in polars are far from being simple dipoles, and the matter does not hit the white dwarf at a single point, but on an accretion arc. So the complicated magnetic field structure near the white dwarf could be responsible for the observed changes in the data of QQ Vul. On the other hand the superposition of the magnetic fields of both stars can lead to a stream geometry deviating from the simple ballistic-magnetic stream model in the case of AM Her.

**Acknowledgments** AS acknowledges partial financial support received from IAU to take part in the IAU Colloquium on MCVs.

#### References

- Davey, S. C., & Smith, R. C. 1996, MNRAS, 280, 481
- Rechenberg, I. 1994, Evolutionsstrategie, Frommann-Holzboog, Stuttgart
- Rutten, R., Dhillon, V., Horne, K., & Kuulkers, E. 1994, A&A, 283, 441
- Schwarz, R., Hedelt, P., Rau, A., Staude, A. & Schwöpe, A.D. in 'The Physics of Cataclysmic Variables and Related Objects', ASP Conference Proceedings, 261, 167
- Schwöpe, A. D., Catalán, M.S., Beuermann, K., Beuermann, K., Metzner, A., Smith, R. C., Steeghs, D., 2000, MNRAS, 313, 533
- Staude, A., Schwarz, R., Schwöpe, A. & Rau, A., 2001, in 'The Physics of Cataclysmic Variables and Related Objects', ASP Conference Proceedings, 261, 680